Proteasome-mediated remodeling of the proteome and phosphoproteome during kiwifruit pollen germination.

Abstract

Proteasome activity is essential for pollen tube emergence and growth; nevertheless, little is known about proteasome function at the molecular level. The objective of this study was to identify molecular targets and pathways which are directly/indirectly controlled by the proteasome during pollen germination. To this aim, changes in the proteome and phosphoproteome of *Actinidia* pollen, germinated in the presence of the proteasome inhibitor MG132, were investigated. Phosphoproteins were enriched by metal oxide/hydroxide affinity chromatography and phosphopeptides were further isolated using titanium ion (Ti^{4+}) functional magnetic microparticles prior to liquid chromatography-tandem mass spectrometry analysis. Our results show that proteasome inhibition affects the phosphoproteome more profoundly than the proteome. Accordingly, the steady-state abundance of some kinases and phosphatases was changed and/or their phosphorylation status altered. Notably, affected proteins are involved in processes that are fundamental to pollen germination such as cytoskeletal organization, vesicular transport, cell wall synthesis and remodeling, protein synthesis, folding and degradation as well as energetic metabolism. Our data provide a molecular framework for the structural alterations observed when the proteasome is inhibited, contribute to the

understanding of how proteasome activity regulates pollen germination, show the cross-talk between phosphorylation and proteasomal degradation and are a resource for further functional analyses.

Significance

Pollen germination and tube growth are fundamental to successful fertilization in seed plants. These events are based on dramatic remodeling and the dismantling of existing programs, which are replaced by new ones. Degradation plays a prominent role in reshaping the protein repertoire, also cross talking with the bulk of post-translational modifications. At present, phosphorylation is the only modification studied in germinating pollen on a large scale. The proteasome has been universally recognized as one of the most important sites for protein degradation and its function has been shown to be essential for pollen tube emergence and elongation. Upon proteasome inhibition structural alterations and dysregulation of pivotal processes governing pollen germination have been described; however, a mechanistic framework for the proteasome function at the molecular level is still lacking. In this investigation we provide the very first view of the global impact of the proteasome in remodeling the proteome and phosphoproteome during germination and tube growth. Our results show how proteasome inhibition alters the levels, and profoundly affects the phosphorylation status of many proteins involved, controlling energetic and synthetic pathways and signaling cascades.

Introduction

Pollen germination and tube growth are dynamic, coordinated processes, essential to sexual reproduction in seed plants. Pollen tubes elongate by tip growth, a mechanism involving vesicle

trafficking [1], actin cytoskeleton organization [2], apical ion flux [3] and cytosolic Ca^{2+} gradients [4]. Identifying the signaling pathways involved in this cellular program has been the focus of intense investigation over the past decade [5]. In recent years, several proteomic analyses have made it possible to establish comprehensive cell-specific protein maps of pollen development [6]. Hundreds of proteins were found to be differentially expressed between mature and germinating pollen grains, most of which are regulated at the transcriptional and/or translational level [7, 8]. Moreover, differential expression patterns between protein isoforms have been detected, likely arising from post-transcriptional and post-translational modification [7, 8].

Extensive protein phosphorylation during anther development has been found in *Arabidopsis* and rice, revealing the important role of this post-translational modification in affecting protein activity [9]. Mayank et al. [10] reported that mature *Arabidopsis* pollen contains many phosphorylated proteins that might be subjected to changes in phosphorylation status upon pollination. Using metal oxide/hydroxide affinity chromatography, Fíla identified 139 [11] and 301 [12] phosphoprotein candidates in tobacco pollen activated *in vitro*. To date, the impact of phosphorylation on pollen tube development has not been fully characterized.

The ubiquitin/proteasome-mediated degradation of proteins plays a pivotal role in both pollen germination and tube growth [13-15]. In this pathway, ubiquitin, an 8.6 kDa protein, is activated and transferred to its substrates via the action of three enzymes: E1, E2, and E3. Although ubiquitin functions as a multivalent signal that can modulate the level, activity and intracellular localization of a protein, ubiquitin-conjugated proteins are usually committed to proteasome degradation [16]. Accordingly, accumulation of ubiquitinated protein was observed in germinating pollen grains after proteasome inhibition [13-15]. On the other hand, for a

significant subset of proteins proteasome degradation can occur independently of ubiquitin conjugation [17]. Thus, proteasome-mediated protein degradation is thought to be a major contributor to the remodeling of the pollen proteome.

Gel-based proteomic analysis revealed 11 unique candidate protein species whose abundance was directly/indirectly regulated by the proteasome during germination in kiwifruit pollen [18]. In the present study, the proteome of kiwifruit pollen germinated in the presence of the proteasome inhibitor MG132 was further analyzed using a gel free proteomic approach to extend our knowledge of the role of the proteasome in remodeling the pollen proteome during germination.

Phosphorylation-triggered degradation is a common strategy for the elimination of regulatory proteins in many important cell signaling processes. The cross talk between phosphorylation and ubiquitin-mediated proteasomal degradation is well established. This cross-regulation is often manifested by the ability of phosphorylation to regulate the ubiquitin conjugating machinery and/or to promote the ubiquitination and degradation of substrates [19]. Ubiquitination can also turn on/off the activity of certain kinases [20]. Examples of proteins where these two post-translational modifications coexist on the same substrate during seed germination have been recently described [21].

Thus, the aim of this study was to analyze how proteasomal degradation control pollen germination modulating both protein abundance and phosphorylation levels.

Materials and methods

Plant material and pollen germination.

Pollen from the male kiwifruit genotype (cv. Tomuri) of *Actinidia deliciosa* var. *deliciosa* [(A. Chev) C. F. Liang et A. R. Ferguson] was collected and managed as described in Vannini et al. [18]. The pollen was rehydrated for 30 min at 30 °C under 100% relative humidity. Germination was performed by suspending the rehydrated pollen grains (1 mg/mL) in liquid medium containing 0.29 M sucrose, 0.4 mM boric acid and 1 mM calcium nitrate. Tube emergence and growth were quantified using the pollen tube growth (PTG) test via photometric determination (A_{500}) [22].

Experimental design.

After rehydration, pollen was transferred to liquid medium containing the proteasome inhibitor MG132 (Selleckchem) to a final concentration of 40 μM. Since the inhibitor was dissolved in dimethyl sulfoxide (DMSO), parallel incubations were set up with DMSO, at the same concentration (0.08%) present in the MG132-treated samples (control). The cultures were incubated for 90 min at 30 °C in the dark. The cells were then collected by Millipore vacuum filtration. Phosphoprotein enrichment with Qiagen column was performed on samples deriving from three different germination experiments with two analytical replicates. Quantification of ubiquitin-conjugated proteins in the phosphoprotein-enriched pool was performed on three biological replicates.

To directly compare proteomic responses to MG132 versus DMSO, four biological replicates were subjected to protein extraction and phosphoprotein enrichment. Four separated metal oxide affinity chromatography (MOAC) and Ti-immobilized metal affinity chromatography (Ti-IMAC) enrichment experiments were carried out. The experimental system is illustrated in Figure 1.

Protein extraction and phosphoprotein enrichment

Phosphorylated proteins were initially isolated from whole pollen extracts using a Phosphoprotein Purification Kit (Qiagen) according to the manufacturer's instructions, with minor modifications. Briefly, pollen samples were suspended in 2 mL of phosphoprotein lysis buffer supplemented with CHAPS, a cocktail of proteasome inhibitors and Benzonase. The cell suspension was homogenized on ice using a Potter-Elvehjem apparatus. After centrifugation, the samples were diluted in loading buffer to a final concentration of 0.1 mg/mL, and 30 mL of the resulting lysate were loaded onto a Qiagen column. Washing and elution were performed as detailed in the manual. Protein concentration was determined using the Bradford assay (BioRad), with serum albumin as a standard. Elution fractions were pooled, concentrated and desalted by ultrafiltration before western immunoblotting analysis.

Alternatively, MG132-treated and DMSO-treated pollen (about 0.4 g vacuum-filtered cells) were suspended 1:10 (w/v) in 10% (w/v) trichloroacetic acid (TCA)/acetone, supplemented with 0.07% (v/v) 2-mercaptoethanol (MSH) and homogenized by a Potter-Elvehjem apparatus [11]. An aliquot of the total protein extract was kept aside for western immunoblotting and proteome analysis (Fig. 1). Enrichment of phosphorylated proteins from total protein extracts was obtained by using metal oxide/hydroxide affinity chromatography, essentially as described by Fíla et al. [11] (Fig. 1).

Electrophoresis and western immunoblotting analysis

Whole protein extracts and phosphoprotein-enriched protein pools from the Qiagen column were resolved by sodium dodecyl sulfate polyacrylamide gel electrophoresis (SDS-PAGE). Gels were

electroblotted onto a nitrocellulose membrane (0.2 µm pore size) (BioRad). The blots were probed with an affinity purified rabbit polyclonal anti-ubiquitin antibody (kindly provided by Prof. A.L. Haas, Department of Biochemistry and Molecular Biology, LSU School of Medicine, New Orleans, Louisiana). Bands were detected using horseradish peroxidase-conjugated secondary antibody (BioRad). Peroxidase activity was revealed with the enhanced chemiluminescence detection method (ECL Plus Kit, Amersham Biosciences).

Protein digestion and Ti-IMAC phosphopeptide enrichment.

Total protein extracts and MOAC-enriched proteins were precipitated by methanol [23], suspended in SDS-buffer (SDS 4% w/v, 100 mM Tris-HCl pH 7.6 and 100 mM DTT) and quantified using a 2D Quant kit (GE Healthcare) using bovine serum albumin as a reference standard. Proteins and phosphoproteins were trypsinized using the Filter Aided Sample Preparation (FASP) method [24] (Fig. 1). Peptides from total protein extracts were directly analyzed by liquid chromatography-tandem mass spectrometry (LC-MS/MS), while phosphopeptides from the MOAC fraction were enriched by MagReSyn Ti-IMAC microbeads (ReSyn Biosciences, Edenvale, Gauteng, South Africa) following the manufacturer's instruction (Fig. 1). All peptides were dried under vacuum and desalted using Zip-Tips (lC18; Millipore) prior to mass spectrometric analysis.

LC−MS/MS analysis and data processing.

The peptides were analyzed in a Q Exactive mass spectrometer as described by Garcia-Seco et al. [25]. Raw data were searched with MaxQuant program (v. 1.5.3.3, http://www.coxdocs.org/doku.php?id=maxquant:start) against the *Actinidia chinensis* protein

163 database (version 2013-02, 39,040 entries) from the International Kiwifruit Genome Consortium
164 (IKGC, http://bioinfo.bti.cornell.edu/cgi-bin/kiwi/home.cgi) and the MaxQuant contaminant list.
165 The search criteria were as follows: two missed cleavages, fixed modification of cysteine
166 (carbamidomethylation), variable modifications of methionine (oxidation), minimum peptide
167 length of six amino acids, precursor mass tolerance was set to 20 ppm for the first search and 4.5
168 ppm for the main search. Phosphorylation on serine, threonine and tyrosine and the addition of
169 diglycine on lysine were added as variable modifications. Label Free Quantification (LFQ),
170 "match between runs" (time window of 0.7 min) and target-decoy search strategy (revert mode)
171 options were enabled. LFQ intensities are the output of the MaxLFQ algorithm [26]. They are
172 based on the (raw) intensities and normalized on multiple levels to ensure that profiles of LFQ
173 intensities across samples accurately reflect the relative amounts of the proteins. A false
174 discovery rate (FDR) of 1% and 2% was accepted for peptide and protein identification,
175 respectively.
176 MaxQuant localization of phosphorylation sites is based on the PTM (post-translational
177 modification) score strategy, which assigns probabilities to each possible phosphorylation site
178 according to its site-determining ions. The identified phosphosites were grouped based on their
179 localization score as described by Olsen et al. [27]: class I ($p > 0.75$), class II ($0.5 < p \leq 0.75$) and
180 class III ($p \leq 0.5$).
181 The raw data ("ProteinGroups", the "Phospho(STY)sites" files) were initially processed using an
182 in-house tool. Incorrect identifications ("Reverse", "One site", and "Contaminant" hits) and not
183 consistent identifications were filtered out: only protein groups or phosphosites detected in at
184 least three of the four biological replicates in almost one analytical group (MG132-treated or
185 control) were considered to assess significant changes. Missing values were estimated from the

dataset based on two criteria for each sample, depending on whether one or more missing values were observed for each entry: when two or three values were available, the missing value was set to a random value within an interval of 1/4 of the entire sample standard deviation centered on the entry average. When only one or no values were available, random values within an interval of 1/4 of the standard deviation of all sample values centered on the global minimum value of all samples in the dataset were imputed. The minimum dataset value and sample standard deviations were determined once before any imputation and applied to all subsequent imputations to avoid drift. Consequently, whole sample standard deviation and dataset minimum value only depended on the starting dataset for each entry calculation.

For the quantitative proteome and phosphoproteome analyses the filtered data were processed with the Perseus software platform (http://www.perseus-framework.org). Log_2 transformed LFQ intensities of protein groups and phosphosites intensities were centered by subtracting the median of the entire set of protein groups LFQ intensities /phosphosite intensities per sample (column). To determine if a change in phosphosite abundance truly reflected the regulation of the phosphorylation status of a protein and not a general change in the abundance of the phosphoprotein, phosphosite intensities levels were normalized to the overall protein abundance [28]: the Log_2 transformed and centered phosphosite intensities were normalized by subtracting the Log_2 transformed and centered LFQ intensities of the corresponding proteins.

The mass spectrometry proteomics data were deposited in the ProteomeXchange Consortium via the PRIDE [29] partner repository with the dataset identifier PXD009100 using the following reviewer account details: Username, reviewer29134@ebi.ac.uk, Password: khSkx0f1.

Downstream bioinformatics analysis.

MaxQuant Output file hits were represented by a group of proteins (group of IDs) sharing the same set or a subset of peptides of the best-match leading protein. For bioinformatics analysis, only the leading protein was considered.

To compare kiwifruit proteins with those of *Arabidopsis*, the *Actinidia* proteins accession numbers were converted into *Arabidopsis* proteins accession numbers using IKGC (http://bioinfo.bti.cornell.edu/cgi-bin/kiwi/home.cgi), with the annotation controlled manually. Functional classification and enrichment analysis were performed using the open-source software package agriGO v. 2.0 (http://systemsbiology.cau.edu.cn/agriGOv2/index.php) and the *Actinidia* protein database from the IKGC as background. SEA (single enrichment analysis) and comparisons were performed using a false discovery rate threshold of 0.01 and 0.05 for the global protein/phosphoprotein datasets and differentially regulated/differentially phosphorylated protein datasets, respectively. Significantly enriched phosphorylation motifs were extracted from class I phosphosites using the open-source program Motif-X (http://motif-x.med.harvard.edu/motif-x.html). The peptide sequences were centered on modification sites (phosphoserine or phosphothreonine) and aligned, including six amino acids up- and downstream of the site of modification. The number of occurrences was set to 20, and the probability threshold was set to $P<10^{-6}$. The IKGC *Actinidia* database was uploaded as background data. Known motifs and probable kinases were searched in the PhosphoMotifFinder (http://www.hprd.org/serine_motifs) database and in the literature [10, 12, 28, 30-32].

Statistical analysis.

Statistical analysis of data was performed using Student's t-test in the GraphPad Prism package.

For proteomic and phosphoproteomic data an Anova based multiple sample test with permutation-based false discovery rate cutoff of 0.05 was performed in the Perseus software in order to analyze the proteins changing in relative abundance and phosphorylation status between analytical groups (MG132-treated and DMSO-treated).

Protein fold change (FC) ratio, expressed as Log_2FC, is defined as the Log_2 of protein abundance in the treatment minus Log_2 protein abundance in the control. Only changes with $Log_2FC \leq -0.6$ or $Log_2FC \geq 0.6$ were considered biologically relevant, respectively.

The Perseus software was also used for principal component analysis (PCA), plot scattering, and hierarchical clustering analysis.

Results

Inhibitory effects of MG132 on pollen germination.

The MG132 concentration of 40 μM was used because significantly inhibits pollen germination and tube growth without inducing cell death [13, 18]. As shown in Fig. S1A, in the presence of 40 μM MG132, tube emergence and elongation decreased by 35%, as previously reported [13, 18]. The marked accumulation of ubiquitin-protein conjugates and the depletion of the ubiquitin monomer confirmed that the ubiquitin proteolytic system was impaired (Fig. S1B).

Total proteomic profiling of Actinidia pollen treated with MG132.

To explore the molecular events controlled by the proteasome during pollen germination and tube growth, we analyzed the total proteome from *Actinidia* pollen treated with MG132 compared with the control.

LC MS/MS analysis and MaxQuant data processing allowed to detect 3300 protein groups (Table S1). Among them, 2169 protein groups were identified in at least three of the four

biological replicates in almost one analytical group (Table S2). The LFQ intensities of the 2169 consistent protein groups were centered, as described in Materials and methods, and considered for further data processing. We performed PCA analysis to point up the relationships among groups of variables indicated in our data set. Figure S2A shows that sample replicates belonging to the same treatment, have been grouped much closer than those exposed to the different treatments (MG132 or DMSO). This result indicates that the effect of proteasome inhibition by MG132 is detectable at the proteome level. The similarities among the samples was also assessed by scatter plotting and determination of the Pearson coefficient. The biological replicates sharing the same treatment revealed an average Pearson correlation of 0.98 (Fig. S2B), indicating that the germination conditions, the chemical treatments and the mass spectrometric analysis were highly reproducible. By contrast, the average correlation value between MG132 and DMSO-treated samples was approximately 0.93, suggesting that MG132 affects the pollen germinating proteome profile. These observations were further confirmed by the clustering analysis. The LFQ intensities were grouped using the hierarchical clustering algorithm of the Perseus software. The experimental groups (MG132- and DMSO-treated samples) are clearly separated according to the expression level in each replicate (Fig. S2C).

Among the 2169 protein groups identified, the statistical analysis revealed that 88 were up- and 61 down-accumulated (Anova multiple sample test, FDR< 0.05, with $Log_2FC \leq -0.6$ or $Log_2FC \geq 0.6$) after proteasome inhibition, corresponding to 6.8% of the total protein groups (Table S3). To assess the quality of our analysis, we compared the 1623 *Arabidopsis* counterparts of our proteome dataset with an atlas of *Arabidopsis* pollen proteins obtained by combining the lists of *Arabidopsis* pollen proteins and transcripts cited in the literature [8, 33]. The comparison

revealed that 1513 (93%) protein species had been previously detected in *Arabidopsis* pollen, whereas 110 have never been reported as pollen-related proteins (Table S4).

MapMan analysis showed that the kiwifruit pollen proteins and the differentially regulated protein species primarily belong to the categories RNA and protein metabolism, metabolism of lipids and amino acid, signaling, cell wall organization and development (Fig. S4). The agriGO SEA analysis showed that the over-represented Gene Ontology (GO) categories in the differentially regulated protein dataset were carbohydrate and protein metabolic processes (Fig. 2).

Proteasome activity regulates the phosphoproteome during kiwifruit pollen germination.

To determine if MG132 affects the phosphoproteome in a quantitative and qualitative manner, we enriched protein extracts obtained from MG132- and DMSO-treated samples using a commercial kit (Qiagen). The amount of proteins recovered in the phosphoprotein enriched pool from MG132-treated samples was 1.5-fold higher than that obtained from the control run in parallel (Fig. 3A).

To gain deeper insight into the effects of proteasome inhibition on the pollen phosphoproteome, we applied a tandem MOAC approach [34] for enrichment of phosphorylated proteins and peptides (Fig. 1). Using this approach, more than 70% of the peptides identified were phosphorylated (1657 out of 2157) compared to the 0.4 % (61 out of 14834) detected in the unenriched samples.

MaxQuant analysis identified 1891 phosphopeptides containing 2095 phosphosites (Table S5). To eliminate false positives, we considered only the phosphosites present in a minimum of three of the four biological replicates in almost one analytical group (MG132-treated or control). We

obtained an analytical set of 1299 unique phosphopeptides containing 1572 phosphosites (Table S6). Of these, 90.3% are phosphoserine (pSer), 9.0% are phosphothreonine (pThr) and 0.7% are phosphotyrosine (pTyr) (Fig. 4A). The intensities of the 1572 consistent phosphosites were centered, as described in Materials and methods.

This dataset was submitted to the PCA analysis. In figure S3A the first principal component (PC1: 79.4%), the second (PC2: 6.5%) and the third (PC3: 4.8%) show the separation between experimental groups (MG132- and DMSO-treated samples) and the similarity of biological replicates. The reproducibility of the phosphopeptide enrichment step was also demonstrated by the average Pearson value of 0.92 obtained among the four biological replicates performed for each treatment. By contrast, the average Pearson correlation value between MG132-treated pollen and the control was 0.52, indicating that proteasome inhibition greatly alters the pollen phosphoproteome (Fig. S3B). The intensities hierarchical clustering (Fig. S3C) confirmed the separation between the experimental groups (MG132- and DMSO-treated samples).

Among the 1572 phosphosites, 1392 (88%) had a localization probability >0.75, indicating that the detection of phosphosites using our strategy is highly robust. The 1572 phosphosites correspond to 711 unique proteins groups (Fig. 4B, Table S6). Most of them (85%) contain one to three phosphosites, 13% contain four to seven phosphosites and 2% contain more than seven phosphosites (to a maximum of 15; Fig. 4C). Among phosphoproteins identified in kiwifruit pollen, 564 share high similarity with *Arabidopsis* proteins (At homologs), 337 (60%) are present in a Phospho atlas (based on the PhosPhat and P3DB databases) and data from Mayank et al. [10] and 227 have never been reported as phosphorylated proteins (Table S7). Our comparison of the 564 At homologs in our phosphoproteome dataset with proteins in the pollen atlas revealed a subset of 52 At homologs not previously reported as pollen proteins (Table S4).

The functional categorization of these phosphoproteins using MapMan revealed an enrichment in the categories protein metabolism, RNA and DNA processing, signaling, and development (Fig. S3). Accordingly, the percentage of transcription factors and kinases/phosphatases was much higher in the phosphoproteome than in the proteome (Fig. 4D).

We subjected our 1572 quantifiable phosphosites to the Anova multiple sample test (Table S6) and we found 405 phosphosites which were significantly different (FDR<0.05) in abundance between MG132 and control samples (Table S8). We did not set a fold change threshold in the analysis of phosphosites because, in our opinion, even small differences in post-translational modifications, if statistically significant, may be relevant from the biological point of view. For 603 phosphosites (out of 1572, in bold in Table S6), we also quantified the matching proteins in the proteome experiment, allowing us to normalize the phosphosite intensities to the abundance of the corresponding total protein (Table S9). The Anova multiple sample test (FDR<0.05) performed onto normalized data revealed that 178 phosphosites were indeed differentially regulated (104 down- and 74 up-accumulated) in terms of phosphorylation status in response to proteasome inhibition (Table S9). Therefore, our differentially phosphorylated protein dataset includes, in addition to the 93 proteins corresponding to these 178 phosphosites, the proteins corresponding to the 258 differentially regulated phosphosites (in red in table S8) for which we failed to identify the corresponding proteins in the total proteome.

The analysis of this differentially phosphorylated protein dataset by using agriGO software showed that the over-represented Gene Ontology (GO) categories were nucleotide and RNA metabolism, cytoskeleton organization, pollen tube development, biological regulation, and spliceosome, among others (Fig. 2).

Motif enrichment and kinases.

Using the Motif-X tool and considering only the high-abundant phosphosites serine (Ser) and threonine (Thr), we searched for the dominant phosphorylation motifs in our phosphoprotein dataset compared with the kiwifruit genome database IKGC (http://bioinfo.bti.cornell.edu/cgi-bin/kiwi/home.cgi) as a background. We identified 39 over-represented phospho motifs, including 29 phospho-Ser motifs and 10 phospho-Thr motifs (Table S10). Eight phospho motifs were enriched by MG132 treatment (shown in red in Table S10). The kinase families that recognize these enriched motifs are: mitogen activated protein kinases (MAPKs), cyclin-dependent protein kinases (CDKs), AGC kinase family protein kinases C/A/G (PKAs/C/G), calcium-dependent protein kinases, receptor-like protein kinases (RLKs), SNF 1-related protein kinases (SnRKs) and casein kinases II (CKII). Several kinases belonging to these families were identified in the kiwifruit pollen proteome and phosphoproteome.

We detected two putative MAP kinases (Achn252431, Achn028141), one CDK (Achn146301), the putative homolog of receptor protein kinase CLAVATA1 (Achn214861) and two RLKs (Achn023871, Achn115291), whose phosphorylation status was regulated by proteasome inhibition. Moreover, one AGCK (Achn069131) and the putative SnRK2 (Achn157571) were regulated in terms of both abundance and phosphorylation status, whereas the regulatory subunit of a putative SnRK1 (Achn365051) was regulated only in terms of protein abundance.

MG132 induces the accumulation of ubiquitin-conjugated proteins in the pollen phosphoprotein pool.

Western analysis with an antibody against ubiquitin revealed the presence of ubiquitinated proteins in the phosphoprotein-enriched pool. Interestingly, there was an almost twofold increase

in the content of ubiquitin conjugates after proteasome inhibition (Fig. 3B), suggesting that, during pollen germination, a portion of the phosphorylated substrates undergoes ubiquitination and subsequent degradation.

After trypsin digestion, the ubiquitin-conjugated proteins release peptides containing a di-glycine fragment covalently attached to the ubiquitinated lysine. We detected 34 ubiquitination sites (Table S11). Among them 22 were unambiguously detected and correspond to 19 proteins (Table S12). Anova multiple sample test (FDR<0.05) revealed that 12 ubiquitination sites (corresponding to 10 phosphoproteins) were differentially regulated (8 up- and 4 down-accumulated) in MG132-treated pollen compared to the control (Table S12). Five of these proteins (Achn111131, Achn200011, Achn222861, Achn304201, and Achn380731) were significantly upregulated in terms of both ubiquitination and phosphorylation. This type of analysis is obviously limited since no enrichment for ubiquitin conjugated proteins was performed, being beyond the scope of the present study; however, it provides evidence that the two post translational modifications can coexist on the same substrate.

Discussion

Inhibition of the proteasome reduces pollen tube emergence and elongation and causes pollen tip swelling and branching, suggesting that proteasome-mediated protein turnover is essential for pollen germination and polarized tube growth [13-15]. In agreement with this observation, both proteasome activity and protein levels of several proteasome subunits have been reported to increase in the germinating with respect to mature quiescent pollen [13, 35]. Although the proteasome is responsible for the degradation of the majority of intracellular proteins, surprisingly MG132 treatment did not cause dramatic changes in total protein abundance,

391 confirming the findings of Vannini et al. [18], and observations made in mammalian cells [36,
392 37]. One possible explanation is that only the steady-state level of short half-life proteins is
393 affected by proteasome inhibition; these polypeptides are usually low-abundant regulatory
394 proteins, hardly detectable within the whole proteome.
395 Interestingly, proteasome inhibition had a greater effect on the pollen phosphoproteome than it
396 did on the total proteome. The simplest reasonable explanation is that this fraction is indeed
397 enriched in proteins with regulatory function which may be subjected to direct or indirect
398 proteasome control.
399 Phosphorylation is an important modification which allows rapid control of the activity of
400 signaling and regulatory proteins [38]. Many studies have demonstrated that proteasome
401 inhibitors can alter signaling pathways and suppress the degradation of multiple phosphorylated
402 signaling molecules [39, 40]. Almost half of the phosphorylation sites identified in our
403 experimental system resulted differentially regulated in terms of phosphorylation status by
404 proteasome inhibition when normalized to total protein levels. Some proteins with multiple
405 phosphorylation sites showed different regulatory trends, providing evidence for the complexity
406 of the effects of proteasome inhibition on phosphorylation patterns during pollen germination
407 (Fig. 5). Accordingly, 14 kinases and 6 phosphatases belonging to MAPK, RLK, CDK, CDPK-
408 SnRKs and PP2C families were found changed in their phosphorylation status after MG132
409 treatment (Table S13). Phosphorylation of MAPK, RLK and CDPK kinase families was found to
410 occur in tobacco pollen during the transition from the quiescent to the activation state [12].
411 Moreover, the phosphorylation motif enrichment analysis onto the differentially phosphorylated
412 protein dataset revealed a significant abundance of [S*PxR] motif recognized by CDKs and
413 [S*P] and [RxxS*] motifs that are typically recognized by MAPKs, AGCkKs, CDPK-SnRKs

414 families and calmodulin/Ca^{2+} kinases (CaMK), further supporting the idea that
415 kinase/phosphatase activity is controlled by the proteasome during pollen germination. Finally,
416 the evidence that six proteins were differentially phosphorylated and ubiquitinated by MG132
417 treatment, suggests a crosstalk between phosphorylation and ubiquitin-mediated proteasome
418 degradation as one of the possible mechanisms through which proteasome activity might affect
419 the phosphoproteome.
420 Relatively little is known about kinase activation/deactivation in pollen germination. Moreover,
421 experimental data directly linking specific kinase activation to their targets have yet to be
422 established. For this reason, it is possible only to speculate about the possible relationships
423 between pollen structural alterations reported in the literature and signaling/regulatory molecular
424 players whose phosphorylation status we found altered upon proteasome inhibition.
425
426 *Cytoskeleton organization.*
427 In *Picea* pollen, MG132 induces depolymerization of F-actin and the disruption of the radial
428 array of cortical microtubules [15]. It has been postulated that this might occur as a consequence
429 of a change in the activity/levels of regulatory proteins. The analysis of the phosphoproteome in
430 MG132-treated kiwifruit pollen suggests that the proteasome may regulate small GTPase-
431 mediated signaling and the activity of actin/microtubule bundling proteins. MG132 indeed
432 interfered with the phosphorylation status of three RLKs (Achn21486, Achn023871 and
433 Achn115291) which are known to phosphorylate GTP-binding proteins, thereby inducing
434 changes in downstream signaling [41, 42]. In *Arabidopsis* pollen tubes, the Rho-like GTPase
435 ROP1 controls F-actin dynamics in cooperation with the ROP-interactive CRIB motif-containing
436 (RIC) proteins RIC4 (F-actin assembly) and RIC3 (F-actin disassembly) [43]. To maintain

polarized growth, the RopGAP protein REN1 interacts with ROP1 and restricts active ROP1 to the apical cap [44]. After MG132 treatment, phosphoprotein species showing sequence similarity to REN1 (Achn265851), RIC3 (Achn342471), RIC5 (Achn342471), RhoGDI 1 (Achn341151), and ARAC7 (Achn312571) exhibited an altered phosphorylation status. In particular, REN1 phosphorylation was reduced, while the RhoGDI phosporylation was increased. Since **p**hosphorylation of REN1 at Ser267 and dephosphorylation of RhoGDI is thought to be essential for protein function [41, 12], both proteins might be inactivated upon proteasome inhibition. Phosphoregulation is an important post-translational modification that modulates the F-actin crosslinking activity of bundling proteins [10, 12, 30, 45, 46]. In the current study, a change in the phosphorylation status of three villin (VLN)-like proteins (Achn268281, Achn380731, Achn09219), one fimbrin-like protein homolog of AtFIM1 (Achn354231), one actin cross-linking protein homolog to Crolin1 (Achn198121) and a homolog of an actin cytoskeleton-regulatory protein (Achn342471) was found in MG132-treated pollen.

Whether the phosphorylation of these proteins promotes or inhibits their activity is unknown. In this regard, Villin1,4 was among the protein species found to accumulate in a phosphorylated and ubiquitinated form following MG132 treatment. Based on this evidence it could be hypothesized that Ser phosphorylation promotes its ubiquitination and subsequent degradation via the proteasome.

Proteins involved in the regulation of microtubule dynamics [47] were also differentially phosphorylated. In particular, MG132 treatment reduced the phosphorylation status of a homolog of the Microtubule Associated Protein 65 (MAP65). CDK phosphorylation of the human MAP65 homolog, has been demonstrated to decrease its bundling activity [48, 49].

Overall, these evidences could at least partly explain the observed altered tip growth and cytoskeleton dynamics when the proteasome function is inhibited.

Vesicular transport.

Polarized pollen tube growth also relies on a fine balance between exocytosis of plasma membrane and cell wall components and endocytosis to recycle excess material [50].

The inhibition of proteasome activity has been shown to cause a disorder in the secretory system which consequently reduces pollen tube growth [15]. In line with this finding, we detected a change in the phosphorylation status of proteins involved in clathrin- and non-clathrin-mediated endocytosis such as one auxillin-like protein (Achn303051), two VHS domain-containing proteins (Achn284791 and Achn046581) and a putative beta subunit of a coatomer protein (Achn199041). The regulation of pollen tube endocytosis through post-translational modifications remains elusive [5]. In mammalian cells, phosphorylation regulates the association and dissociation cycle of the clathrin-based endocytic machinery. Dephosphins are coordinately dephosphorylated during endocytosis of synaptic vesicles; notably, blocking dephosphorylation is known to inhibit endocytosis [51].

Alteration in the phosphorylation status of kiwifruit protein species homologous to *Arabidopsis* Type I inositol-1,4,5-trisphosphate 5-phosphatase-like (IP5P12) and phosphatidyl-myo-inositol-4,5-bisphosphate phosphatase SAC2, suggests that phosphoinositides (PIs) homeostasis could be affected as well by proteasome inhibition. Phosphoinositides are asymmetrically distributed among diverse endomembranes and function as signaling compounds [52, 53]. PI phosphatases and kinases help generate and maintain the gradients required for endomembrane trafficking, cell wall deposition and the control of growth polarity in plants [54]. IP5P12 controls Ins(1,4,5)P3

and Ca^{2+} levels and is crucial for maintaining pollen dormancy and for regulating early pollen germination [55]. SAC2 hydrolyzes the 5-phosphate of PtdIns(3,5)P_2 to form PtdIns3*P*, which has been implicated in vacuolar morphology. Interestingly, the overexpression of SAC phosphatases results in vacuoles larger than those of the control [56], similar to the vacuolar phenotype induced by MG132 treatment in *Picea* pollen [15].

In the differentially phosphorylated protein dataset, we identified few protein species with a Pleckstrin homology (PH) domain that can bind to phosphoinositides, including Achn231821 (homologous to dynamin-2A [DRP2B]), Achn314541 (homologous to sorting nexin 2B [SNX2B]), and Achn204251 (homologous to AtPDK1). DRP2B binds specifically to PtdIns3P and is involved in clathrin-mediated vesicle trafficking from the trans-Golgi to the central vacuole [57, 58]. SNX2B plays a role in vesicular protein sorting [59]. AtPDK1 might couple lipid signals to phosphorylation of the activation loops of several protein kinases of the so-called AGC kinase family.

An increase in the phosphorylation of an oxysterol binding protein (OSBP, Achn180551), and a VAP (vesicle-associated protein, Achn205791) was observed in kiwifruit pollen after MG132 treatment. These proteins seem to be involved in sterol trafficking at the endoplasmic reticulum and Golgi interface in plants [60]. In human cells, the Golgi localization of OSBP is regulated by phosphorylation mediated by a Protein Kinase D [61].

At the protein level, the inhibition of the proteasome induced the over-accumulation of VPS28-1 (Achn344941), a component of the ESCRT-I complex, as well as a putative nexin (Achn073251) involved in vesicular protein sorting and the putative vesicle-trafficking protein SEC22b (Achn360671). Conversely, the levels of the exocyst complex component Sec6 (Achn202541),

504 protein transport protein SEC31 (Achn134681) and a putative transducin family protein/WD-40
505 (Achn320091) were decreased.
506 All these results suggest that altered vesicular trafficking induced by MG132 may be the
507 consequence not only of the disruption of cytoskeletal dynamics, but also to changes in the level
508 and/or activity of proteins involved in vesicle transport, exocytosis and endocytosis.
509
510 *Cell wall synthesis and remodeling***.**
511 Sheng et al. [15] reported a sharp decline in cell wall components in pollen tubes treated with
512 MG132 with respect to the control, probably due to the inhibition of vesicle transport and/or to
513 the altered turnover of enzymes associated with cell wall synthesis and remodeling. Consistent
514 with the latter hypothesis, the steady-state level of both cellulose synthase and pectin
515 methylesterases (PMEs) significantly decreased in kiwifruit pollen after the same treatment.
516 Cellulose plays an important role in stabilizing the pollen tube tip wall [62]. Pectins, are
517 increasingly de-esterified by PMEs in the areas away from the tip to provide mechanical support
518 to the distal area of the elongating tubes [63]. Thus, alterations in the levels of cellulose and
519 pectins would explain the apical swelling of the pollen tube and the enlargement of tube
520 diameters [14].
521 The observed down-accumulation of arabinogalactan proteins (AGPs) could also play a role in
522 this process. Indeed, inhibition of AGP function results in tube shortening and malformation in
523 kiwifruit pollen [64].
524
525 *Protein synthesis, folding and degradation***.**

Inhibition of the proteasome by MG132 reduces the levels of newly synthesized proteins in mammalian, yeast and plant cells [65-69]. This effect seems to be mediated by the phosphorylation of initiation factor Eif2 and Eif4 [65-67]. In our experimental system, MG132 treatment altered the phosphorylation status of some proteins bearing strong similarity to the initiation factors Eif4-like (Achn390151, Achn009851, Achn052611, and Achn295641), eiF2 (Achn293871 and Achn080441), the TAF4-like factor (Achn299451) and eIF3 (Achn239121). Pollen germination and tube elongation depend on continuous protein synthesis [70]. Therefore, the impairment of protein synthesis may at least in part explain the inhibitory effect of MG132 on germination and tube elongation.

In *Picea* pollen tubes, MG132 induces dilation of the endoplasmic reticulum (ER), vacuolization of the cytoplasm and the accumulation of ubiquitinated proteins, especially near the ER membrane [15]. The chaperone protein CDC48 is an essential factor that is extensively involved in ERAD (ER-associated degradation) [71]. In mammalian and yeast cells, CDC48 recognizes multi-ubiquitin moieties on many proteins and targets them to the proteasome [72, 73]. Serine phosphorylation of CDC48 leads to its reduced association with ubiquitinated proteins, thus promoting their degradation [74]. Interestingly, we found that MG132 treatment reduced the phosphorylation of a putative CDC48 (Achn03736). In addition, we detected increased phosphorylation of a protein homologous to CDC48-interacting UBX-domain protein (PUX1), which regulates AtCDC48 by inhibiting its ATPase activity and promoting the disassembly of the active hexamer [75]. It could be speculated that proteasome inhibition creates a negative feedback loop, leading to a reduction in CDC48 activity to slow the release of ubiquitinated proteins to the proteasome. Moreover, the retrograde translocation of misfolded proteins from the ER has been shown to be dependent on functioning cytosolic proteasomes [76]. Thus, treatment

549 of cells with proteasome inhibitors results in the accumulation of misfolded proteins within the
550 endoplasmic reticulum. Reduced phosphorylation of calreticulin homologous to AtCALR1
551 (Achn260371) was found in MG132-treated pollen samples. This protein is a Ca^{2+}-binding
552 molecular chaperone that facilitates the folding of newly synthesized glycoproteins and regulates
553 Ca^{2+} homeostasis in the ER lumen [77]. Phosphorylation/dephosphorylation events have been
554 postulated to control and modulate the biological activity of the protein. In particular, Trotta et
555 al. [78] have demonstrated that calreticulin is dephosphorylated by PP2A. Knocking down PP2A
556 resulted in a strong calreticulin phosphorylation and misregulation of genes involved in the UPR
557 (Unfolded Protein Response). Thus, dephosphorylation of calreticulin under MG132 treatment
558 could stimulate its activity as a chaperon to relieve the ER stress induced by proteasome
559 inhibition. Notably, a PP2A regulatory subunit TAP46 (Achn046981) was among the
560 phosphorylated proteins accumulated in MG132-treated pollen. Since phosphorylation may
561 promote PP2A activity [79], it could be hypothesized that this event may be responsible for
562 calreticulin dephosphorylation.
563 Changes in the phosphorylation of a putative E2 ubiquitin-conjugating enzyme (Achn389631),
564 two E3 ubiquitin-protein ligase RING1-like proteins (Achn245461, Achn126221) and one EIN3-
565 binding F-box protein 1 (Achn195831) were detected in MG132-treated kiwifruit pollen.
566 Phosphorylation can regulate E2 and E3 ligase activity [19]. Thus, the inhibition of the
567 proteasome could regulate ubiquitin ligase activity by inducing a change in their phosphorylation
568 status. Finally, we detected an increase in the abundance of proteasome subunits RPN10
569 (Achn159691) and RPN13-like (Achn368911). Interestingly, the RPN10 subunit mediates the
570 autophagic degradation of the proteasome following MG132 treatment, presumably to remove
571 inactive particles [80].

572 Among the differentially phosphorylated proteins in MG132-treated pollen, one over-represented
573 GO category was RNA splicing. Reversible protein phosphorylation plays a key role in
574 spliceosome assembly and the catalytic steps of splicing [81]. Our data indicate that the
575 proteasome participates in splicing events during the early phases of pollen germination via
576 changes in the phosphorylation status of spliceosome components. Although the early stages of
577 pollen germination and early tube growth largely depend on pre-synthesized mRNA, the
578 appearance of many novel transcripts during pollen germination has been demonstrated [82].
579 Indeed, several phosphoproteins involved in transcription whose phosphorylation status was
580 altered upon proteasome inhibition, such as transcription factors and RNA binding proteins, were
581 detected. Overall, our data indicate that protein degradation via the proteasome regulates not
582 only the translation of mRNA already present in the pollen, but also of newly synthesized RNAs.
583
584 *Energetic metabolism***.**
585 In *Picea,* MG132 strongly disturbs mitochondrial remodeling and significantly reduces the
586 mitochondrial membrane potential [15]. In the present study, the levels and the phosphorylation
587 status of proteins involved in mitochondrial protein import was affected by MG132 treatment. In
588 particular, levels of TOM 20 (Achn238661) and the phosphorylation status of TOM 22
589 (Achn246651) were altered after MG132 treatment. Notably, TOM 22 phosphorylation controls
590 the import and assembly of the TOM complex [83, 84]. Moreover, reduced protein levels of a
591 putative LETM1 (Achn034101) were found. LETM1 (leucine zipper-EF-hand-containing
592 transmembrane protein 1) is a mitochondrial proton/calcium antiporter required for the
593 maintenance of tubular shape and cristae organization in pollen tubes [85]. These observations

further support the evidence that upon proteasome inhibition the bioenergetic function of mitochondria is impaired.

Conclusions

Data reported in this paper provide the first global view of how proteasome activity directly/indirectly contributes to the proteome and, particularly, to phosphoproteome remodeling during pollen germination. The changes in the levels and/or in the phosphorylation status of several regulatory protein species outline a molecular framework which could explain the structural alterations observed under conditions of proteasome inhibition (Fig. 6). They also shed light on the molecular players within energetic/synthetic pathways and signaling cascades which are sensitive to an impairment in proteasome function.

References

[1] L. Zonia, T. Munnik, Vesicle trafficking dynamics and visualization of zones of exocytosis and endocytosis in tobacco pollen tubes, J. Exp. Bot., 59 (2008) 861-873.

[2] C.D. Justus, P. Anderhag, J.L. Goins, M.D. Lazzaro, Microtubules and microfilaments coordinate to direct a fountain streaming pattern in elongating conifer pollen tube tips, Planta, 219 (2004) 103-109.

[3] E. Michard, F. Alves, J.A. Feijó, The role of ion fluxes in polarized cell growth and morphogenesis: the pollen tube as an experimental paradigm, Int. J. Dev. Biol., 53 (2009) 1609-1622.

[4] P.K. Hepler, L. Vidali, A.Y. Cheung, Polarized cell growth in higher plants, Annu. Rev. Cell Dev. Biol., 17 (2001) 159-187.

[5] Y. Guan, J. Guo, H. Li, Z. Yang, Signaling in pollen tube growth: crosstalk, feedback, and missing links, Mol. Plant, 6 (2013) 1053-1064.

[6] Z. Zhang, M. Hu, X. Feng, A. Gong, L. Cheng, H. Yuan, Proteomes and Phosphoproteomes of Anther and Pollen: Availability and Progress, Proteomics, 17 (2017).

[7] S. Dai, T. Wang, X. Yan, S. Chen, Proteomics of pollen development and germination, J. Proteome Res., 6 (2007) 4556-4563.

[8] P. Chaturvedi, A. Ghatak, W. Weckwerth, Pollen proteomics: from stress physiology to developmental priming, Plant Reprod., 29 (2016) 119-132.

[9] J. Ye, Z. Zhang, C. You, X. Zhang, J. Lu, H. Ma, Abundant protein phosphorylation potentially regulates *Arabidopsis* anther development, J. Exp. Bot., 67 (2016) 4993-5008.

[10] P. Mayank, J. Grossman, S. Wuest, A. Boisson-Dernier, B. Roschitzki, P. Nanni, T. Nühse, U. Grossniklaus, Characterization of the phosphoproteome of mature *Arabidopsis* pollen, Plant J., 72 (2012) 89-101.

[11] J. Fíla, A. Matros, S. Radau, R.P. Zahedi, V. Čapková, H.P. Mock, D. Honys, Revealing phosphoproteins playing role in tobacco pollen activated *in vitro*, Proteomics, 12 (2012) 3229-3250.

[12] J. Fíla, S. Radau, A. Matros, A. Hartmann, U. Scholz, J.L. Feciková, H.P. Mock, V. Čapková, R.P. Zahedi, D. Honys, Phosphoproteomics Profiling of Tobacco Mature Pollen and Pollen Activated in vitro, Mol. Cell. Proteomics, 15 (2016) 1338-1350.

[13] A. Speranza, V. Scoccianti, R. Crinelli, G.L. Calzoni, M. Magnani, Inhibition of proteasome activity strongly affects kiwifruit pollen germination. Involvement of the ubiquitin/proteasome pathway as a major regulator, Plant Physiol., 126 (2001) 1150-1161.

[14] V. Scoccianti, E. Ovidi, A.R. Taddei, A. Tiezzi, R. Crinelli, L. Gentilini, A. Speranza, Involvement of the ubiquitin/proteasome pathway in the organisation and polarised growth of kiwifruit pollen tubes, Sex. Plant Reprod., 16 (2003) 123-133.

[15] X. Sheng, Z. Hu, H. Lü, X. Wang, F. Baluška, J. Šamaj, J. Lin, Roles of the ubiquitin/proteasome pathway in pollen tube growth with emphasis on MG132-induced alterations in ultrastructure, cytoskeleton, and cell wall components, Plant Physiol., 141 (2001) 1578-1590.

[16] B. Sharma, D. Joshi, P.K. Yadav, A.K. Gupta, T.K. Bhatt, Role of ubiquitin-mediated degradation system in plant biology, Front. Plant Sci., 7 (2016) 806. doi: 10.3389/fpls.2016.00806.

[17] J. Erales, P. Coffino, Ubiquitin-independent proteasomal degradation, Biochim. Biophys. Acta, 1843 (2014) 216-221.

[18] C. Vannini, M. Bracale, R. Crinelli, V. Marconi, P. Campomenosi, M. Marsoni, V. Scoccianti, Proteomic analysis of MG132-treated germinating pollen reveals expression signatures associated with proteasome inhibition, PLoS One, 9 (2014) e108811. doi: 10.1371/journal.pone.0108811.

[19] T. Hunter, The age of crosstalk: phosphorylation, ubiquitination, and beyond, Mol. Cell, 28 (2007) 730-738.

[20] J.A. Witowsky, G.L. Johnson, Ubiquitylation of MEKK1 inhibits its phosphorylation of MKK1 and MKK4 and activation of the ERK1/2 and JNK pathways, J. Biol. Chem., 278 (2003) 1403-1406.

[21] I. Ruiz-Ballesta, G. Baena, J. Gandullo, L. Wang, Y.M. She, W.C Plaxton, C. Echevarría, New insights into the post-translational modification of multiple phosphoenolpyruvate carboxylase isoenzymes by phosphorylation and monoubiquitination during sorghum seed development and germination, J. Exp. Bot., 67 (2016) 3523-3536.

[22] U. Kristen, R. Kappler, The pollen tube growth test, Methods Mol Biol, 43 (1995) 189-198.

[23] M. Marsoni, M. Bracale, L. Espen, B. Prinsi, A.S. Negri, C. Vannini, Proteomic analysis of somatic embryogenesis in *Vitis vinifera*, Plant Cell. Rep., 27 (2008) 347-356.

[24] J.R. Wiśniewski, M. Mann, Consecutive proteolytic digestion in an enzyme reactor increases depth of proteomic and phosphoproteomic analysis, Anal. Chem., 84 (2012) 2631-2637.

[25] D. Garcia-Seco, M. Chiapello, M. Bracale, C. Pesce, P. Bagnaresi, E. Dubois, L. Moulin, C. Vannini, R. Koebnik, Transcriptome and proteome analysis reveal new insight into proximal and distal responses of wheat to foliar infection by *Xanthomonas translucens*, Sci. Rep., 7 (2017).

[26] J. Cox, M.Y. Hein, C.A. Luber, I. Paron, N. Nagaraj, M. Mann, Accurate proteome-wide label-free quantification by delayed normalization and maximal peptide ratio extraction, termed MaxLFQ, Mol. Cell. Proteomics, 13 (2014) 2513-2526.

[27] J.V. Olsen, B. Blagoev, F. Gnad, B. Macek, C. Kumar, P. Mortensen, M. Mann, Global, *in vivo*, and site-specific phosphorylation dynamics in signaling networks, Cell, 127 (2006) 635-648.

[28] L.D. Vu, E. Stes, M. Van Bel, H. Nelissen, D. Maddelein, D. Inzé, F. Coppens, L. Martens, K. Gevaert, I. De Smet, Up-to-date workflow for plant (phospho)proteomics identifies differential drought-responsive phosphorylation events in maize leaves, J. Proteome Res., 15 (2016) 4304-4317.

[29] J.A. Vizcaíno, A. Csordas, N. del-Toro, J.A. Dianes, J. Griss, I. Lavidas, G. Mayer, Y. Perez-Riverol, F. Reisinger, T. Ternent, Q.W. Xu, R. Wang, H. Hermjakob, Update of the PRIDE database and its related tools, Nucleic Acids Res., 44 (2016) D447-456.

[30] Q. Chao, Z.F. Gao, Y.F. Wang, Z. Li, X.H. Huang, Y.C. Wang, Y.C. Mei, B.G. Zhao, L. Li, Y. B. Jiang, B.C. Wang, The proteome and phosphoproteome of maize pollen uncovers fertility candidate proteins, Plant Mol. Biol., 91 (2016) 287-304.

[31] L.L. Lin, C.L. Hsu, C.W. Hu, S.Y. Ko, H. L. Sieh, H.F. Huang, Integrating Phosphoproteomics and bioinformatics to study brassinosteroid-regulated phosphorylation dynamics in *Arabidopsis*, BMC Genomics, 16 (2015) 533. doi: 10.1186/s12864-015-1753-4.

[32] D.W. Lv, X. Li, M. Zhang, A.Q. Gu, S.M. Zhen, C. Wang, X.H. Li, Y.M. Yan, Large-scale phosphoproteome analysis in seedling leaves of *Brachypodium distachyon* L, BMC Genomics, 15 (2014) 375. doi: 10.1186/1471-2164-15-375.

[33] N. Rutley, D. Twell, A decade of pollen transcriptomics, Plant Reprod., 28 (2015) 73-89.

[34] W. Hoehenwarter, M. Thomas, E. Nukarinen, V. Egelhofer, H. Röhrig, W. Weckwerth, U. Conrath, G.J. Beckers, Identification of novel *in vivo* MAP kinase substrates in *Arabidopsis thaliana* through use of tandem metal oxide affinity chromatography, Mol. Cell. Proteomics, 12 (2013) 369-380.

[35] S. Dai, T. Chen, K. Chong, Y. Xue, S. Liu, T. Wang, Proteomics identification of differentially expressed proteins associated with pollen germination and tube growth reveals characteristics of germinated *Oryza sativa* pollen, Mol. Cell. Proteomics, 6 (2007) 207-230.

[36] W. Kim, E.J. Bennett, E.L. Huttlin, A. Guo, J. Li, A. Possemato, M.E. Sowa, R. Rad, J. Rush, M.J. Comb, J.W. Harper, S.P. Gygi, Systematic and quantitative assessment of the ubiquitin-modified proteome, Mol. Cell, 44 (2011) 325-340.

[37] D.L. Swaney, P. Beltrao, L. Starita, A. Guo, J. Rush, S. Fields, N.J. Krogan, J. Villén, Global analysis of phosphorylation and ubiquitylation cross-talk in protein degradation. Nat. Methods, 10 (2013) 676-682.

[38] E.K. Day, N.G.Sosale, M.J. Lazzara, Cell signaling regulation by protein phosphorylation: a multivariate, heterogeneous, and context-dependent process, Curr. Opin. Biotechnol. 40 (2016) 185-192.

[39] D.M. Schewe, J.A, Aguirre-Ghiso, Inhibition of eIF2alpha dephosphorylation maximizes bortezomib efficiency and eliminates quiescent multiple myeloma cells surviving proteasome inhibitor therapy, Cancer Res., 69 (2009) 1545-1552.

[40] L. Kubiczkova, L. Pour, L. Sedlarikova, R. Hajek, S. Sevcikova, Proteasome inhibitors - molecular basis and current perspectives in multiple myeloma, J. Cell. Mol. Med. 18 (2014) 947-961.

[41] D.Wengier, I. Valsecchi, M.L. Cabanas, W.H. Tang, S. McCormick, J. Muschietti, The receptor kinases LePRK1 and LePRK2 associate in pollen and when expressed in yeast, but dissociate in the presence of style extract, Proc. Natl. Acad. Sci. U.S.A., 100 (2003) 6860-6865.

[42] A.Y. Cheung, H.M. Wu, Structural and signaling networks for the polar cell growth machinery in pollen tubes, Annu. Rev. Plant Biol., 59 (2008) 547-572.

[43] Y. Gu, Y. Fu, P. Dowd, S. Li, V. Vernoud, S. Gilroy, Z. Yang, A Rho family GTPase controls actin dynamics and tip growth via two counteracting downstream pathways in pollen tubes, J. Cell Biol., 169 (2005) 127-138.

[44] C. Craddock, I. Lavagi, Z. Yang, New insights into Rho signaling from plant ROP/Rac GTPases, Trends Cell Biol., 22 (2012) 492-501.

[45] Y. Miao, X. Han, L. Zheng, Y. Xie, Y. Mu, J.R. Yates, D.G. Drubin, Fimbrin phosphorylation by metaphase Cdk1 regulates actin cable dynamics in budding yeast, Nat. Commun., 7 (2016) 11265. doi: 10.1038/ncomms11265.

[46] J.Z. Chen, J. Fürst, M.S Chapman, N. Grigorieff, Low-resolution structure refinement in electron microscopy, J. Struct. Biol., 144 (2003) 144-151.

[47] G. Komis, P. Illés, M. Beck, J. Šamaj, Microtubules and mitogen-activated protein kinase signalling, Curr. Opin. Plant Biol., 14 (2011) 650-657.

[48] W. Jiang, G. Jimenez, N.J. Wells, T. J. Hope, G.M. Wahl, T. Hunter, R. Fukunaga, PRC1: a human mitotic spindle-associated CDK substrate protein required for cytokinesis, Mol. Cell, 2 (1998) 877-885.

[49] C. Mollinari, J.P. Kleman, W. Jiang, G. Schoehn, T. Hunter, R. L. Margolis, PRC1 is a microtubule binding and bundling protein essential to maintain the mitotic spindle midzone, J. Cell Biol., 157 (2002) 1175-1186.

[50] R.M. Parton, S. Fischer-Parton, M.K.Watahiki, A.J. Trewavas, Dynamics of the apical vesicle accumulation and the rate of growth are related in individual pollen tubes, J. Cell Sci., 114 (2001) 2685-2695.

[51] M.A. Cousin, P.J. Robinson, The dephosphins: dephosphorylation by calcineurin triggers synaptic vesicle endocytosis, Trends Neurosci., 24 (2001) 659-665.

[52] M.L. Simon, M. P. Platre, S. Assil, R. van Wijk, W.Y. Chen, J. Chory, M. Dreux, T. Munnik, Y. Jaillais, A multi-colour/multi-affinity marker set to visualize phosphoinositide dynamics in *Arabidopsis*, Plant J., 77 (2014) 322-337.

[53] J.E. Vermeer, T. Munnik, Using genetically encoded fluorescent reporters to image lipid signalling in living plants, Methods Mol Biol., 1009 (2013) 283-289.

[54] I. Heilmann, Phosphoinositide signaling in plant development, Development, 143 (2016) 2044-2055.

[55] Y. Wang, Y.J. Chu, H.W. Xue, Inositol polyphosphate 5-phosphatase-controlled Ins(1,4,5)P3/Ca2+ is crucial for maintaining pollen dormancy and regulating early germination of pollen, Development, 139 (2012) 2221-2233.

[56] P. Nováková, S. Hirsch, E. Feraru, R. Tejos, R. van Wijk, T. Viaene, M. Heilmann, J. Lerche, R. De Rycke, M.I. Feraru, P. Grones, M. Van Montagu, I. Heilmann, T. Munnik, J. Friml, SAC phosphoinositide phosphatases at the tonoplast mediate vacuolar function in *Arabidopsis*. Proc. Natl. Acad. Sci. U.S.A., 111 (2014) 2818-2823.

[57] M. Fujimoto, S. Arimura, T. Ueda, H. Takanashi, Y. Hayashi, A. Nakano, N. Tsutsumi, *Arabidopsis* dynamin-related proteins DRP2B and DRP1A participate together in clathrin-coated vesicle formation during endocytosis, Proc. Natl. Acad. Sci. U.S.A., 107 (2010) 6094-6099.

[58] W.F. Boss, A.J. Davis, Y.J. Im, R.M. Galvao, I.Y. Perera, in: Majumder AL, BB, B. (Eds.), Biology of Inositols and Phosphoinositides, Springer US 2006.

[59] N.Q. Phan, S.J. Kim, D.C. Bassham, Overexpression of *Arabidopsis* sorting nexin AtSNX2b inhibits endocytic trafficking to the vacuole, Mol. Plant, 1 (2008) 961-976.

[60] R.S. Saravanan, E. Slabaugh, V.R. Singh, L.J. Lapidus, T. Haas, F. Brandizzi, The targeting of the oxysterol-binding protein ORP3a to the endoplasmic reticulum relies on the plant VAP33 homolog PVA12, Plant J., 58 (2009) 817-830.

[61] S. Nhek, M. Ngo, X. Yang, M.M. Ng, S.J. Field, J.M. Asara, N.D. Ridgway, A.Toker, Regulation of oxysterol-binding protein Golgi localization through protein kinase D-mediated phosphorylation, Mol. Biol. Cell, 21 (2010) 2327-2337.

[62] L. Aouar, Y. Chebli, A. Geitmann, Morphogenesis of complex plant cell shapes: the mechanical role of crystalline cellulose in growing pollen tubes, Sex. Plant Reprod., 23 (2010) 15-27.

[63] L.-Q.Chen, D. Ye, Roles of Pectin Methylesterases in Pollen-Tube Growth, J. Integ. Plant Biol., 49 (2007) 94-98.

[64] A. Speranza, A.R. Taddei, , G. Gambellini, E. Ovidi, V. Scoccianti, The cell wall of kiwifruit pollen tubes is a target for chromium toxicity: alterations to morphology, callose pattern and arabinogalactan protein distribution, Plant Biol. (Stuttg), 11 (2009) 179-193.

[65] J.L. Cowan, S.J. Morley, The proteasome inhibitor, MG132, promotes the reprogramming of translation in C2C12 myoblasts and facilitates the association of hsp25 with the eIF4F complex, Eur. J. Biochem., 271 (2004) 3596-3611.

[66] Q. Ding, E. Dimayuga, W.R. Markesbery, J.N. Keller, Proteasome inhibition induces reversible impairments in protein synthesis, FASEB J., 20 (2006) 1055-1063.

[67] A. Yerlikaya, S.R. Kimball, B.A. Stanley, Phosphorylation of eIF2 alpha in response to 26S proteasome inhibition is mediated by the haem-regulated inhibitor (HRI) kinase, Biochem. J., 412 (2008) 579-588.

[68] A. Suraweera, C. Münch, A. Hanssum, A. Bertolotti, Failure of amino acid homeostasis causes cell death following proteasome inhibition, Mol. Cell, 48 (2012) 242-253.

[69] D. Van Hoewyk, Use of the non-radioactive SUnSET method to detect decreased protein synthesis in proteasome inhibited *Arabidopsis* roots, Plant Methods, 12 (2016) 20. doi: 10.1186/s13007-016-0120-z.

[70] H. Hao, Y. Li, Y. Hu, J. Lin, Inhibition of RNA and protein synthesis in pollen tube development of Pinus bungeana by actinomycin D and cycloheximide, New Phytol., 165 (2005) 721-729.

[71] H. Meyer, M. Bug, S. Bremer, Emerging functions of the VCP/p97 AAA-ATPase in the ubiquitin system, Nat. Cell Biol., 14 (2012) 117-123.

[72] E. Rabinovich, A. Kerem, K.U. Fröhlich, N. Diamant, S. Bar-Nun, AAA-ATPase p97/Cdc48p, a cytosolic chaperone required for endoplasmic reticulum-associated protein degradation, Mol. Cell. Biol., 22 (2002) 626-634.

[73] G.H. Baek, H. Cheng, V. Choe, X. Bao, J.Shao, S. Luo, H. Rao, Cdc48: a swiss army knife of cell biology, J. Amino Acids, 2013 (2013) 183421. doi: 10.1155/2013/183421.

[74] J.B. Klein, M.T. Barati, R. Wu, D. Gozal, L.R. Jr, Sachleben, H. Kausar, J.O. Trent, E. Gozal, M.J. Rane, Akt-mediated valosin-containing protein 97 phosphorylation regulates its association with ubiquitinated proteins, J. Biol. Chem., 280 (2005) 31870-31881.

[75] D.M. Rancour, S. Park, S.D. Knight, S.Y. Bednarek, Plant UBX domain-containing protein 1, PUX1, regulates the oligomeric structure and activity of *Arabidopsis* CDC48, J. Biol. Chem., 279 (2004) 54264-54274.

[76] B. Tsai, Y. Ye, T.A. Rapoport, Retro-translocation of proteins from the endoplasmic reticulum into the cytosol, Nat. Rev. Mol. Cell Biol., 3 (2002) 246-255.

[77] X.Y. Jia, L.H. He, R.L. Jing, R.Z. Li, Calreticulin: conserved protein and diverse functions in plants, Physiol. Plant., 136 (2009) 127-138.

[78] A. Trotta, G. Konert, M. Rahikainen, E.M. Aro, S. Kangasjärvi, Knock-down of protein phosphatase 2A subunit B'γ promotes phosphorylation of CALRETICULIN 1 in *Arabidopsis thaliana*, Plant Signal. Behav., 6 (2011) 1665-1668.

[79] J.H. Ahn, T. McAvoy, S.V. Rakhilin, A. Nishi, P. Greengard, A.C.Nairn, Protein kinase A activates protein phosphatase 2A by phosphorylation of the B56delta subunit, Proc. Natl. Acad. Sci. U.S.A., 104 (2007) 2979-2984.

[80] R.S. Marshall, F. Li, D.C. Gemperline, A.J. Book, R.D. Vierstra, Autophagic Degradation of the 26S Proteasome Is Mediated by the Dual ATG8/Ubiquitin Receptor RPN10 in *Arabidopsis*, Mol. Cell, 58 (2015) 1053-1066.

[81] T. Misteli, D.L.Spector, RNA polymerase II targets pre-mRNA splicing factors to transcription sites in vivo. Mol. Cell, 3 (1999) 697-705.

[82] Y. Wang, W.Z. Zhang, L.F. Song, J.J. Zou, Z. Su, W-H. Wuet, Transcriptome analyses show changes in gene expression to accompany pollen germination and tube growth in *Arabidopsis*, Plant Physiol., 148 (2008) 1201-1211.

[83] A.B. Harbauer, M. Opalińska, C. Gerbeth, J.S. Herman, S. Rao, B. Schönfisch, B. Guiard, O. Schmidt, N. Pfanner, C. Meisinger, Mitochondria. Cell cycle-dependent regulation of mitochondrial preprotein translocase, Science, 346 (2014) 1109-1113.

[84] C. Gerbeth, O. Schmidt, S. Rao, A.B. Harbauer, D. Mikropoulou, M. Opalińska, B. Guiard, N. Pfanner, C. Meisinger, Glucose-induced regulation of protein import receptor Tom22 by cytosolic and mitochondria-bound kinases, Cell Metab., 18 (2013) 578-587.

[85] B. Zhang, C. Carrie, A. Ivanova, R. Narsai, M.W. Murcha, O. Duncan, Y. Wang, S.R. Law, V. Albrecht, B. Pogson, E. Giraud, O. Van Aken, J. Whelan, LETM proteins play a role in the accumulation of mitochondrially encoded proteins in *Arabidopsis thaliana* and AtLETM2 displays parent of origin effects, J. Biol. Chem., 287 (2012) 41757-41773.

Figures

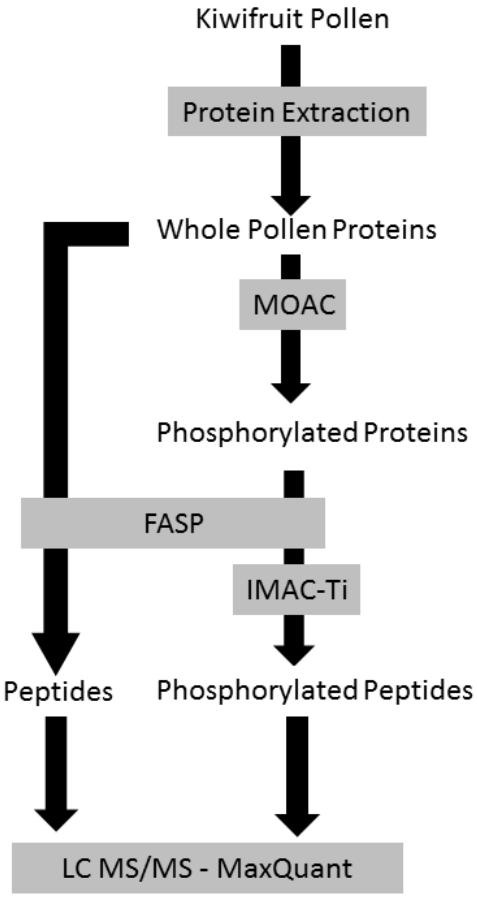

Fig. 1. Workflow of proteomics experiments. Kiwifruit pollen treated with DMSO or MG132 was subjected to total protein extraction. An aliquot of the whole protein extract was FASP digested for proteome analysis; the remaining sample was used for phosphoprotein enrichment. Phosphoproteins were enriched by MOAC, FASP digested and phosphopeptides were further isolated by a Ti-IMAC based chromatography. Peptides and phosphopeptides were identified and quantified by LC MS/MS analysis.

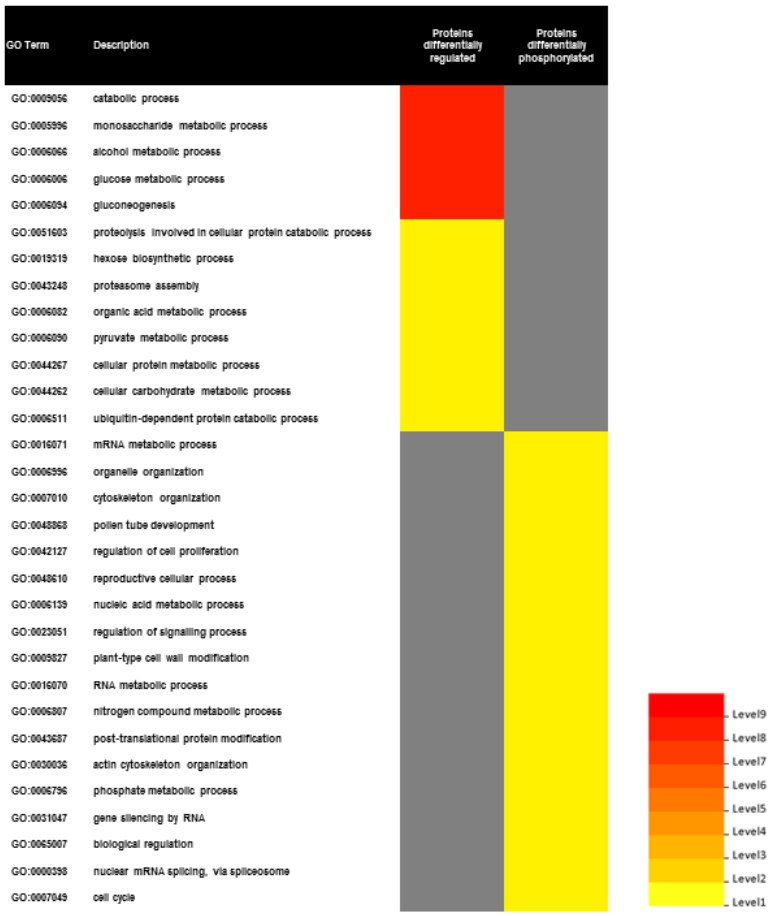

Fig. 2. Gene ontology enrichment for biological process of differentially regulated and differentially phosphorylated proteins. The analysis was performed in batch for both protein datasets using the Single Enrichment Analysis (SEA) agriGO tool. SEA results were compared using SEA compare tool. The image contains the most relevant gene ontology (GO) significant terms (FDR threshold 0.05). Box color represents significance, ranging from dark red (most significant) to light yellow (least significant).

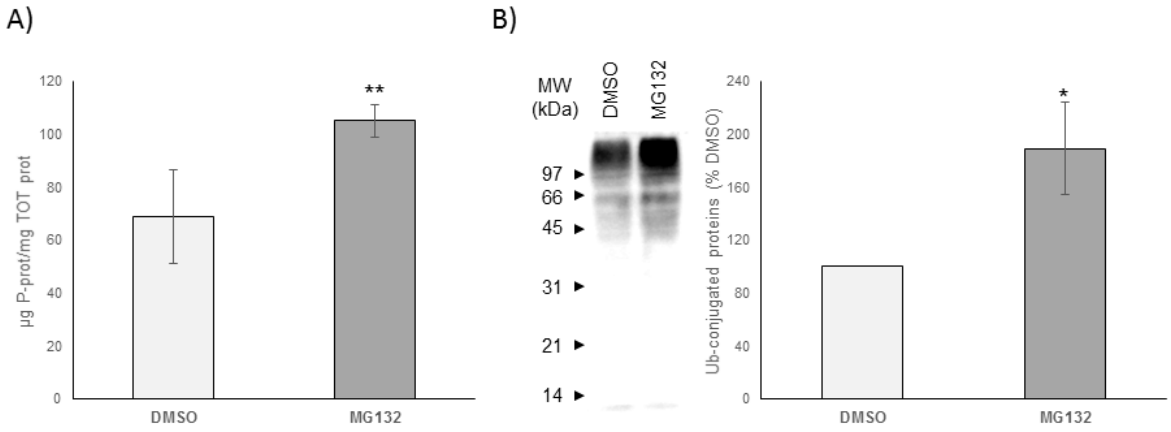

Fig. 3. Accumulation of proteins and ubiquitin-conjugated proteins within the phosphoprotein-enriched pool in MG132-treated pollen. (A) 3 mg of proteins were subjected to phosphoprotein enrichment using the Qiagen kit. Protein content in the eluate was determined by the Bradford assay and expressed as µg of proteins in the enriched fraction (P-prot) per mg of total proteins. Bars represent the average value ± SD. (B) Twenty µg of phosphorylated proteins were resolved in SDS-PAGE and immunoblotted with an anti-ubiquitin antibody. A representative image is shown. Quantification of ubiquitin-protein conjugates was performed in a Chemi Doc system (BioRad) and expressed as % of DMSO-treated sample. Bars represent the average value ± SD is shown. Statistical analysis was performed on densitometric values. *$p<0.05$; **$p<0.01$ vs DMSO control.

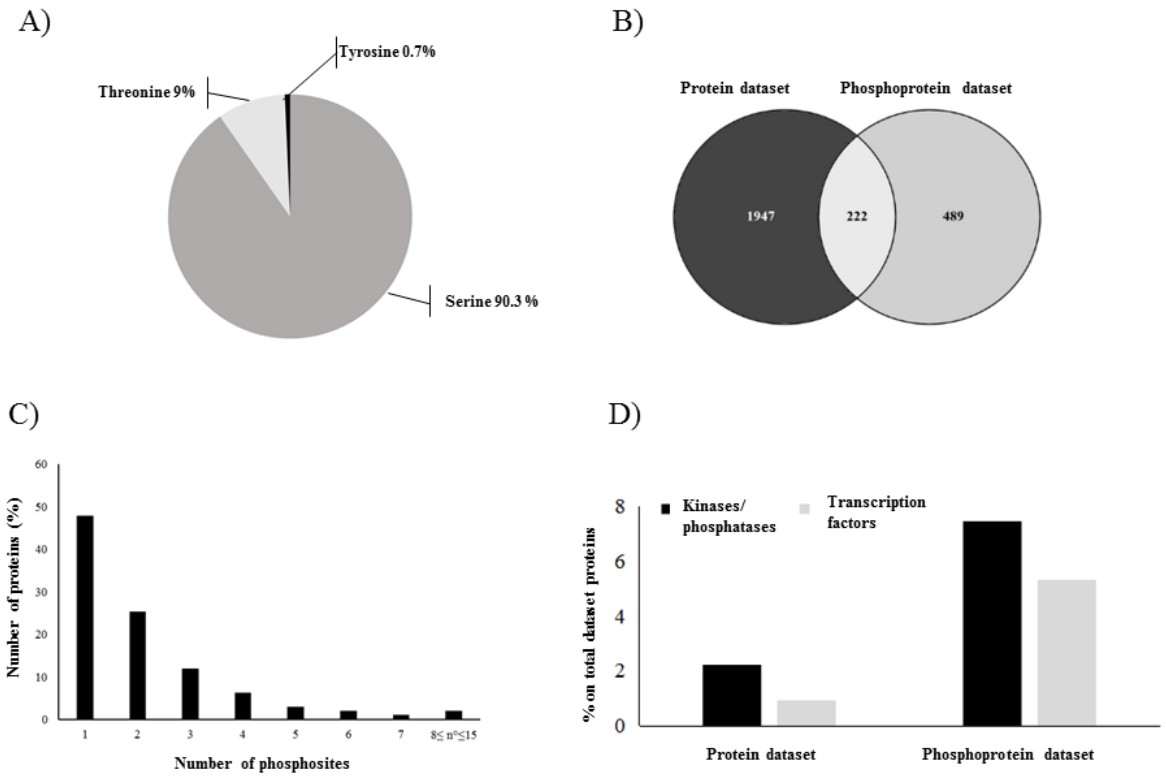

Fig. 4. A) Number of phosphorylation sites according to the phosphorylated amino acid (serine, threonine and tyrosine) identified. B) Number of protein species unambiguously identified in the proteome and phosphoproteome analysis. C) Percentage of identified proteins in relation to the number of phosphosites found on the same protein group. D) Number of kinases, phosphatases and transcription factors identified in the protein and phosphoprotein datasets expressed as a percentage of the total number of identified proteins.

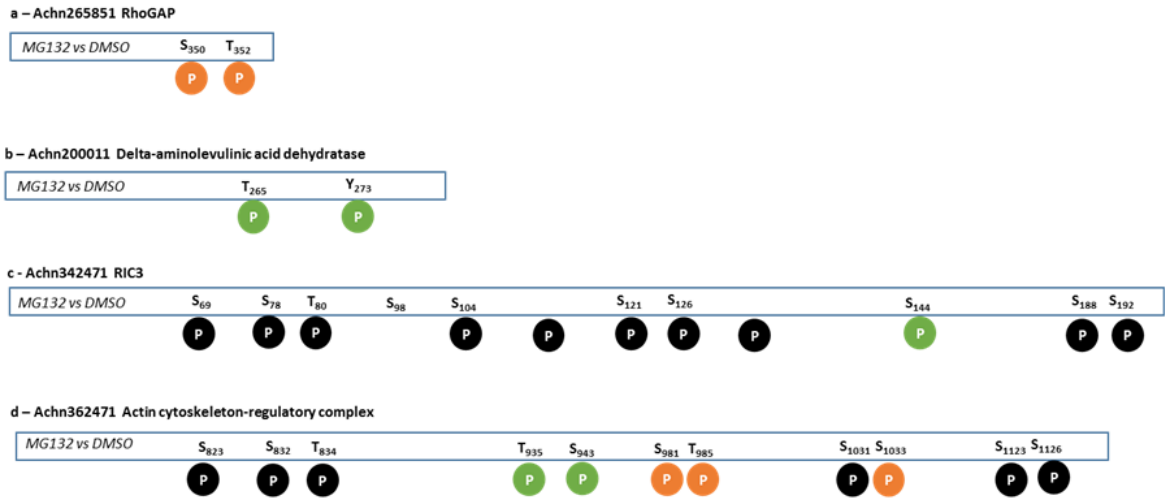

Fig. 5. Phosphorylation patterns of four selected phosphoproteins identified in our dataset. "S", "T" and "Y" stands for serine, threonine and tyrosine, respectively; the numbers indicate the position of the post translational modification in the protein sequences. "P" in the circle indicates unchanged (black), up-regulated (green) and down-regulated (orange) phosphosites after MG132 treatment.

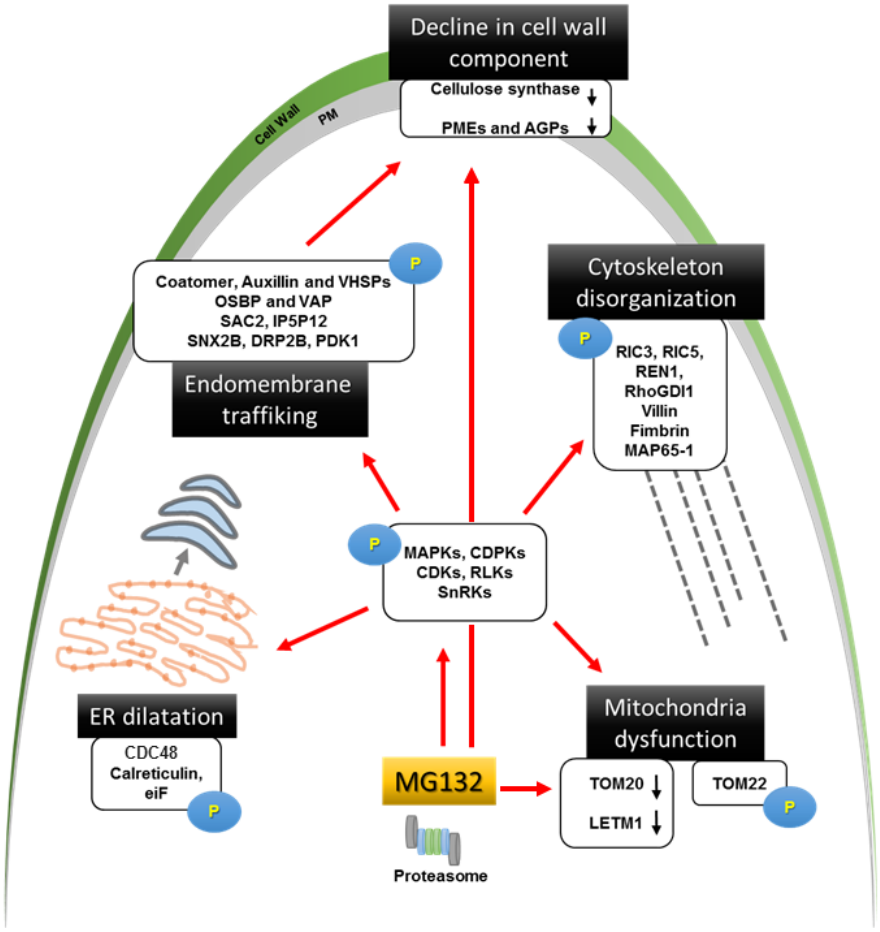

Fig. 6. Schematic model summarizing the molecular players involved in the structural alterations associated with proteasome inhibition in kiwifruit pollen. P: proteins changing in their phosphorylation level; arrows: proteins changing in their abundance.